A Two-level Traffic Light Control Strategy for Preventing Incident-Based Urban Traffic Congestion

Liang Qi, *Student Member, IEEE*, MengChu Zhou, *Fellow, IEEE*, and WenJing Luan, *Student Member, IEEE*

***Abstract*— This work designs a two-level strategy at signalized intersections for preventing incident-based urban traffic congestion by adopting additional traffic warning lights. The first-level one is a ban signal strategy that is used to stop the traffic flow driving toward some directions, and the second-level one is a warning signal strategy that gives traffic flow a recommendation of not driving to some directions. As a visual and mathematical formalism for modeling discrete-event dynamic systems, timed Petri nets are utilized to describe the cooperation between traffic lights and warning lights, and then verify their correctness. A two-way rectangular grid network is modeled via a cell transmission model. The effectiveness of the proposed two-level strategy is evaluated through simulations in the grid network. The results reveal the influences of some major parameters, such as the route-changing rates of vehicles, operation time interval of the proposed strategy, and traffic density of the traffic network on a congestion dissipation process. The results can be used to improve the state of the art in preventing urban road traffic congestion caused by incidents.**

***Index Terms*— Timed Petri net (TPN), discrete event system, cell transmission model (CTM), traffic light control, emergency strategy, congestion formation and dissipation, traffic incident.**

I. Introduction

With a growing number of vehicles in many countries, traffic congestion becomes a serious problem and has spread like a plague from major metropolitan areas to numerous small to mid-size cities. It increases human travel time, fuel consumption and air pollution. The current research [1] finds that a congestion can be caused by one of the following three reasons: 1) a temporary obstruction within a traffic network such as an incident, 2) a permanent capacity constraint, and 3) a stochastic fluctuation in the demand. Note that the incident-based congestion is a traffic jam that can cause large-scale congestion to the upstream traffic flow if the incident is not cleared in a timely fashion. The rapid developments in communications and computing technologies promote several advanced traffic control strategies to deal with these problems [2]–[8].

Among those strategies, the traffic light control at road intersections is regarded as a major strategy to guarantee the safe crossing of conflicting streams of vehicles and pedestrians and lead to efficient network operations [8]. Much work has been done to develop various traffic signal strategies for promoting traffic efficiency. They are mainly categorized as fixed-timed, traffic responsive, and predictive control strategies. The first one is widely adopted in most current urban traffic systems due to its easy implementation and low management cost. However, its drawbacks are that the resulting settings are based on historical rather than real-time data. The second one, such as SCOOT [9] and SCATS [10], is based on measured current traffic states and has been effectively used in many cities around the world [8]. Dotoli *et al.* [11] propose a discrete-time-model-based signal timing plan and show its effectiveness in dealing with severe traffic congestion. The third one is a model-based optimization control strategy that can forecast the future traffic behavior of the network based on traffic-forecasting models [12]. Traffic light strategies can be designed for single-intersection control and network-wide control. For a single signalized intersection, an optimal traffic light switching scheme can be computed efficiently to minimize the queue lengths described by a model [13]. Recently, there are some researches about the network-wide traffic control [14]–[22]. Aboudolas *et al.* [14], [15] propose a real-time signal control methodology based on a store-and-forward modeling paradigm by analytically solving a quadratic-programming problem that aims at minimizing and balancing the link queues. Geroliminis *et al.* [18], Ramezani *et al.* [19], Haddad *et al.* [20], Ji and Geroliminis [21], and Haddad and Geroliminis [22] obtain many theoretic results of a macroscopic fundamental diagram that can be utilized to establish efficient and elegant strategies to control network flows.

Most of the above theories and strategies are suitable for non-saturated and stable traffic conditions. However, changing environmental conditions in a non-predictable way such as an incident may lead to an invalidation of the above traffic light control strategies, and causes traffic jam or unexpected congestion. To solve this problem, route guidance and driver information systems can be employed to improve the network efficiency via direct or indirect recommendation of alternative

Manuscript received January 10, 2016; revised May 13, 2016 and July 20, 2016; accepted October 28, 2016. Date of publication December 30, 2016; date of current version December 26, 2017. This work was supported in part by the National Natural Science Foundation of China under Grants 61202028 and 61374148, and in part by the Scholarship from the China Scholarship Council. The Associate Editor for this paper was N. Geroliminis. *(Corresponding author: MengChu Zhou.)*

L. Qi and W. Luan are with the College of Electronics and Information Engineering, Tongji University, Shanghai 201804, China (e-mail: qiliangsdkd@163.com; wenjingmengjing@163.com).

M. Zhou is with the Key Laboratory of Embedded System and Service Computing, Ministry of Education, Tongji University, Shanghai 201804, China and also with the Department of Electrical and Computer Engineering, New Jersey Institute of Technology, Newark, NJ 07102 USA (e-mail: zhou@njit.edu).

Color versions of one or more of the figures in this paper are available online at http://ieeexplore.ieee.org.

Digital Object Identifier 10.1109/TITS.2016.2625324

routes [8]. The real-time traffic information can be sent to drivers through two kinds of devices: in-car [17] or road-side devices [2]. The first one, such as radio and GPS-navigator, helps drivers make sensible routing decisions at bifurcation nodes of the network. However, drivers who are familiar with the traffic conditions in a network may not use such devices and optimize their individual routes based on their past experience. The second one includes electronic signs displayed on roadways which provide present travel time, traffic congestion and special events. For example, Orlando-Orange County Expressway Authority in Florida added 29 fixed dynamic message signs (DMS) to their toll road network between 2006 and 2008 for traffic diversion [2]. Al-Deek *et al.* [2] discuss the role of traffic information provided by DMS. Though such devices can provide comprehensive information, they usually have great management cost and increase the drivers' decision-making complexity. Currently DMS is mainly installed on some arterial highways.

So far incident-based urban traffic congestion is mostly controlled and prevented through traffic flow diversion with the help of the traffic police. Ban signals are usually adopted [23], [24] so as to notify road users of a ban situation that might not be readily apparent otherwise. In many countries, ban signs take the shape of an equilateral triangle with a white background and a thick red border. These strategies are unfortunately labor-intensive, inflexible and non-intelligent. This work proposes to adopt additional traffic warning lights for sending incident or congestion warnings. These lights can be easily installed at signalized intersections and are divided into two kinds: ban signals and warning ones. Their use and cooperation with traditional traffic lights at road intersections yield a novel and more flexible two-level emergency strategy for preventing traffic congestion caused by incidents. This work proposes to utilize timed Petri nets (TPNs) [25], [26] for the design of traffic light control strategies: normal one using normal traffic lights and emergency one using warning lights. Through these TPN-based formal models, it successfully verifies the correctness of the control systems. The strategy can consequently be implemented directly with hardware and software co-design. Note that the reason to adopt PNs is their graphical and mathematical representation ability to describe well the cooperation of traffic lights [27]–[34]. Recently, some studies use PNs to model the highway traffic [35] and signalized traffic intersections [36]–[39] in a microscopic way.

In order to better understand the dissipation of traffic congestion, many researchers have explored its formation. They perform that through simulation by adopting an accident as an obstruction in their traffic network model. Some simulation models are proposed in [1] and [23], which concentrate on a holistic view of traffic jam formation due to various incidents. Wright and Roberg [1] propose an incident-based jam growth model and discuss the impact of the length of the channelized part of roads and stopline width assignment on jam formation. Roberg *et al.* [40] develop several alternative strategies to prevent the gridlock of a network and dissipate traffic jams once they have formed. Long *et al.* [24] have extended a cell transmission model (CTM) and applied it to simulate

Fig. 1. A traffic light set.

incident-based jam propagation in two-way rectangular grid networks. They also propose control strategies for dispersing incident-based traffic jam and evaluate their efficiency. Compared with the traffic flow models utilized in one-way networks [23], [40], CTM can simulate network-wide traffic flow in a more realistic manner. Furthermore, two-way roads are more commonly found in urban traffic networks than one-way ones. In this work, the proposed strategy is evaluated through a simulation study in a two-way rectangular grid network modeled via an extended CTM. The impact of route-changing rate of vehicles owing to traffic warning lights is investigated and the effectiveness of the proposed strategy is evaluated. Besides, because of the real-time requirement of the operation and the hard-measurability of an accident, the impact of strategy's start and stop time on traffic jam formation and dissipation is investigated.

The rest of this paper is organized as follows. Section II presents a signalized intersection and traffic light control model via TPNs. Section III gives a two-level traffic light control strategy and performs its correctness verification. Section IV presents a two-way rectangular grid network modeled with an extended CTM, and then evaluates the effectiveness of the proposed two-level strategy via simulation. Section V concludes this paper.

II. Traffic Light Control

This section aims to describe the traffic light phase transitions at signalized intersections, and build the normal traffic light control strategy based on TPNs.

A. Traffic Lights

We assume that each of the four directions north ($\boldsymbol{n}$), east ($\boldsymbol{e}$), south ($\boldsymbol{s}$), and west ($\boldsymbol{w}$) deploys a traffic light set. As shown in Fig. 1, each set includes 9 lights that have the capacity of sending seven kinds of traffic light signals: a red one (R), three yellow ones with a left turn arrow (YL), a straight arrow (YS), and a right turn arrow (YR), and three green ones with a left turn arrow (GL), a straight arrow (GS), and a right turn arrow (GR), respectively. In our work we deploy a four-phase traffic light rule to direct the traffic flow at a signalized intersection as shown in Fig. 2. The phase transition forms a cycle, i.e., from phases a to d, and then back to a. For convenience, X_n, Y_e, Z_s, and W_w are denoted as traffic lights along directions $\boldsymbol{n}$, $\boldsymbol{e}$, $\boldsymbol{s}$, and $\boldsymbol{w}$, respectively, where X, Y, Z, $W \in \{R, YS, YL, YR, GS, GL, GR\}$. The detailed operations are described next and modeled by a TPN model. For convenience, in the following discussion, let $\chi \in \{\boldsymbol{n}, \boldsymbol{e}, \boldsymbol{s}, \boldsymbol{w}\}$, $\xi \in \{\boldsymbol{n}, \boldsymbol{s}\}$, and $\zeta \in \{\boldsymbol{e}, \boldsymbol{w}\}$.

B. Traffic Light Control Model

Traffic light control systems with traffic light phase transitions are regarded as discrete event systems. In order to ensure

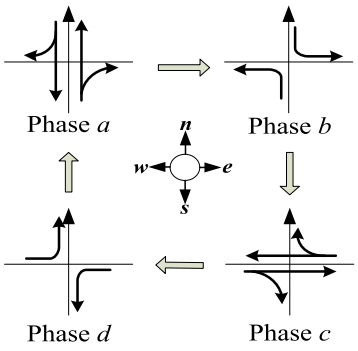

Fig. 2. Four phase transitions of the traffic control system.

such systems to be correctly implemented by the co-design of hardware and software, we first use TPN as a formal model to perform its design.

PNs [25], [26], [40]–[43] are a type of bipartite directed graphs with four types of objects, i.e., places, transitions, directed arcs connecting places to transitions and transitions to places, and inhibitor arcs from places to transitions. Deterministic delays associated with PN transitions lead to TPNs [25], [26]. In TPNs, each transition t is attached with a fixed enabling time duration $\tau(t)$. If t becomes enabled, then it fires after time duration $\tau(t)$. If $\tau(t) \neq 0$, t is called a deterministic transition. If $\tau(t) = 0$, t is called an immediate transition and fires at the moment when it becomes enabled. Graphically, immediate and deterministic transitions are drawn by thin and thick black bars, respectively. An inhibitor arc links place p to t with a small circle attached to t. It prevents t from firing as long as p is marked if $(p, t) \in H$. In the model in this paper, we specify that each arc has a weight of 1 and the capacity of each place is 1 (i.e., the net is 1-bounded or safe [26]). For convenience, let G denote the global time and G_0 the initial time. When a TPN model is built, we can construct its reachability graph by following the firing rules [26]. The graph size can be reduced by attaching to each arc a sequence of transitions containing only one deterministic transition. Note that if more than one deterministic transition fires at the same time, they are attached to the same corresponding arc and are put in a parenthesis. Now we use TPNs to construct a normal traffic light control strategy.

In our discussion, the traffic light control policy for a signalized intersection satisfies the following statements [31]:

- The order of traffic lights forms a complete cycle;
- The policy starts when all red lights are on;
- A yellow duration is adopted during the light transition from green light to red one; and
- To insure traffic safety, all red lights are on when the light transition is completed.

Fig. 3 presents the TPN model of a normal traffic light strategy. Table I describes the meanings of places and transitions with their enabling durations. Note that we assume such time durations for an illustration purpose. They can be changed to user-desired values based on a real-time traffic condition. This will not affect the control structure of the strategy. Let G_0=0

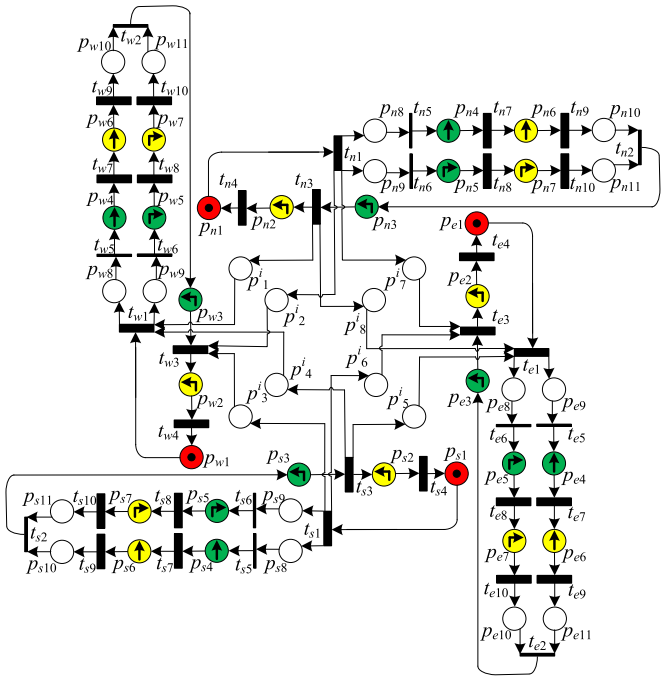

Fig. 3. TPN model of a normal traffic light control strategy at intersection I^i.

TABLE I

MEANINGS OF TRANSITIONS AND PLACES AND TRANSITION DELAYS OF FIG. 3

P	Meaning	T	Meaning	τ(s)
$p_{\chi 1}$	R	$t_{\chi 1}$	Changing R to GS and GR	4
$p_{\chi 2}$	YL	$t_{\chi 7}$ and $t_{\chi 8}$	Changing GS and GR to YS and YR, respectively	15
$p_{\chi 3}$	GL	$t_{\chi 9}$ and $t_{\chi 10}$	Changing YS and YR to GL	2
$p_{\chi 4}$	GS	$t_{\chi 3}$	Changing GL to YL	10
$p_{\chi 5}$	GR	$t_{\chi 4}$	Changing YL to R	2
$p_{\chi 6}$	YS	others	Immediate ones with no meaning but for a control purpose	
$p_{\chi 7}$	YR			
$p_{\chi 6}$-$p_{\chi 9}$, p^i_1-p^i_8	No meaning but for a control purpose			

at the initial state of the TPN, i.e., only $p_{\chi 1}$ contains a token at G_0. $t_{\xi 1}$ is enabled and fires after 4 seconds such that a token is moved from $p_{\xi 1}$ and each of $p_{\xi 8}$ and $p_{\xi 9}$ obtains a token. At this time, $t_{\xi 5}$ and $t_{\xi 6}$ are enabled. Given $\tau(t_{\xi 5})$=$\tau(t_{\xi 6})$=0, both transitions fire immediately resulting that each of $p_{\xi 4}$ and $p_{\xi 5}$ obtain a token and each of p^i_2, p^i_3, p^i_6, and p^i_7 obtains a token, thus enabling $t_{\xi 7}$ and $t_{\xi 8}$. It denotes that the lights change from R_ξ to GR_ξ and GS_ξ and the duration time of GR_ξ and GS_ξ are 15 seconds because $\tau(t_{\xi 7}) = \tau(t_{\xi 8}) = 15$. $t_{\xi 7}$ and $t_{\xi 8}$ fire at G=20 such that tokens are moved from $p_{\xi 4}$ and $p_{\xi 5}$ to $p_{\xi 6}$ and $p_{\xi 7}$, respectively. This denotes that the lights change from GR_ξ and GS_ξ to YR_ξ and YS_ξ and the duration time of YR_ξ and YS_ξ are 3 seconds. After that, $t_{\xi 9}$ and $t_{\xi 10}$ fire such that tokens are moved from $p_{\xi 6}$ and $p_{\xi 7}$ to $p_{\xi 10}$ and $p_{\xi 11}$, respectively. The immediate transition $t_{\xi 2}$ is enabled and fires by removing the tokens in $p_{\xi 10}$ and $p_{\xi 11}$ and depositing a token to $p_{\xi 3}$. This means that the traffic lights GL_ξ are turning on at G=21 and the duration time of GL_ξ is 10 seconds since $\tau(t_{\xi 3})$=10. Then the light changes from GL_ξ to Y_ξ at G=31, i.e., $t_{\xi 3}$ fires with a token removed

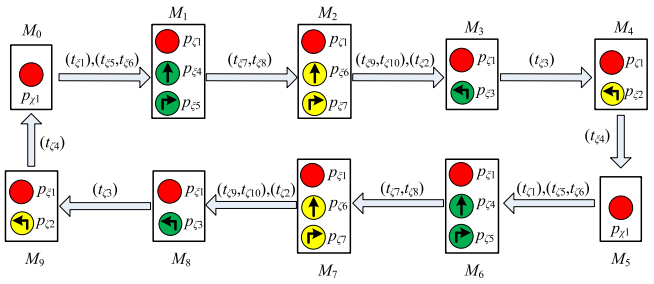

Fig. 4. The reachability graph of the model in Fig. 3.

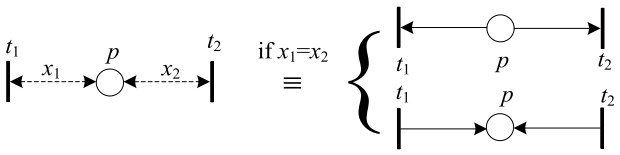

Fig. 5. A dotted double sided arrow.

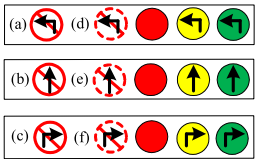

Fig. 6. Three ban signal lights and three warning ones installed with the traffic lights at intersection I^i: (a) $b^i_{\chi,L}$, (b) $b^i_{\chi,S}$, (c) $b^i_{\chi,R}$, (d) $w^i_{\chi,L}$, (e) $w^i_{\chi,S}$, and (f) $w^i_{\chi,R}$.

from $p_{\xi 3}$ in $p_{\xi 2}$. At the same time, a token is filled into each of p^i_1, p^i_4, p^i_5, and p^i_8. Then $t_{\xi 4}$ with $\tau(t_{\xi 4})$=2 and $t_{\zeta 1}$ with $\tau(t_{\zeta 1})$=4 are enabled and fire at G=33 and G=35, respectively. It means that the duration time of YL_ξ is 2 seconds. Note that, $t_{\xi 1}$ is not enabled at G=35 because each of 1-capacitied places p^i_2, p^i_3, p^i_6 and p^i_7 contains a token. Then the traffic lights successively turn to GS_ζ and GR_ζ, YS_ζ and YR_ζ, GL_ζ, YL_ζ, and back to their initial states when G=63. Then $t_{\xi 1}$ fires at G=65, and the same transition firing sequence is executed repeatedly. For convenience, we denote markings of the TPN as the states of the lights, and have M_0=(R_ξ, R_ζ), M_1=(GS_ξ, GR_ξ, R_ζ),M_2=(YS_ξ, YR_ξ, R_ζ), M_3=(GL_ξ, R_ζ), M_4=(YL_ξ, R_ζ), M_5=(R_ξ, R_ζ), M_6=(GS_ζ, GR_ζ, R_ξ), M_7=(YS_ζ, YR_ζ, R_ξ), M_8=(GL_ζ, R_ξ), and M_9=(YL_ζ, R_ξ). The reachability graph of the TPN model is shown in Fig. 4. Since this graph containing all transitions is a finite circle, the TPN model is live and reversible. The time necessary to complete a cycle from marking M_i, $i \in \mathrm{N}^+$ to itself is 60 seconds except that from M_0 to M_0 for the first time which is 63 seconds. The proposed model makes sure that the order of the traffic lights forms a cycle. It directs the traffic light phases operating in a cycle "$a \to b \to c \to d \to a$". Note that M_1 and M_5 are not same because token counts in $p^i_1 - p^i_8$ are different.

III. A Two-Level Strategy

Based on the normal traffic light control strategy proposed in the previous section, we use TPNs to design traffic light control strategies at intersections to deal with incidents and prevent their induced traffic congestion. Such traffic light control strategies are called emergency ones. They need some additional lights, i.e., ban lights and warning ones. The proposed emergency strategy is divided into two levels: a ban signal strategy and a warning signal one. When it is executed, a ban signal strategy adopting ban lights can stop the traffic flow driving towards some directions and a warning signal strategy adopting warning lights gives traffic flow a recommendation of not driving to certain directions. The cooperation among normal traffic lights and warning lights are modeled and verified with TPNs.

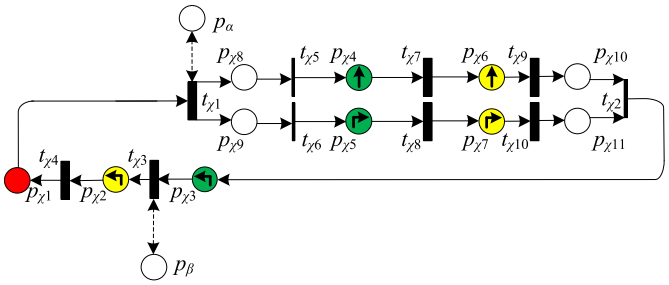

Fig. 7. The TPN model of a strategy for direction χ extracted from Fig. 3.

Now we present the two-level emergency traffic light control strategy at intersection I_i by using TPNs. We first define dotted double sided arrows that connect several transitions with one place as shown in Fig. 5 where each arrow is attached with an integer $x > 0$. Dotted double sided arrows with the same x represent the arcs that have the same direction, i.e., both from transitions to the place or from the place to transitions. For example, in Fig. 5, if $x_1 = x_2$ and one arc is from t_1 to p (respectively, from p to t_1), then another is from t_2 to p (respectively, from p to t_2). The traffic light control strategy from direction χ is drawn in Fig. 7. The following discussion is about the control strategies extended from the one in Fig. 7.

A. Warning Lights

We deploy two kinds of warning sign facilities named warning lights at intersections for sending warning signals to vehicles. In fact, they are installed besides traffic lights at intersections. They can be divided into two sets, and each set has three lights, as shown in Fig. 6. The straight, left and right ban signal lights are denoted by $b^i_{\chi,L}$, $b^i_{\chi,S}$, and $b^i_{\chi,R}$, giving a ban signal to vehicles that intend to turn left, drive straight and turn right at the upstream of I^i, respectively; the warning signal lights are denoted by $w^i_{\chi,L}$, $w^i_{\chi,S}$, and $w^i_{\chi,R}$, to warn vehicles that intend to turn left, drive straight and turn right at the upstream of I^i, respectively. Thus, when some road links from I^i are interrupted, the lights can ban or warn vehicles that attempt to enter the downstream conflict sections. For simplicity, $b^i_{\chi,S}$, $b^i_{\chi,L}$, $b^i_{\chi,R}$, $w^i_{\chi,S}$, $w^i_{\chi,L}$, and $w^i_{\chi,R}$ are also used to denote places in the following TPN models. In the following discussions, the traffic light strategies that adopt warning lights are called emergency ones.

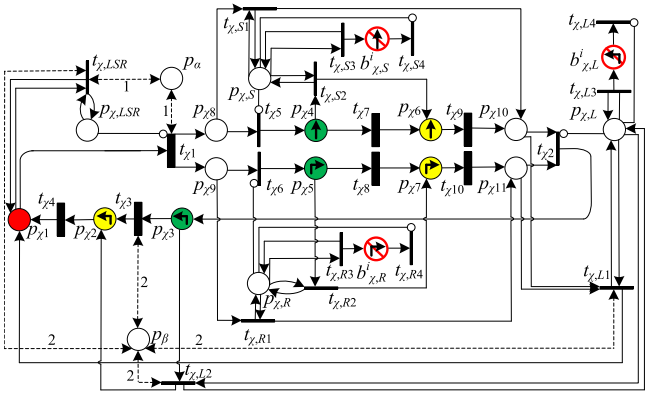

Fig. 8. The TPN model of strategy I.

B. Level-I Strategy

The *Level-I* emergency traffic light control strategy adopting ban signal lights is designed via a TPN as shown in Fig. 8, where p_α, $p_\beta \in \{p_1^i - p_8^i\}$, and $(p_\alpha, t_{\chi 1})$ and $(p_\alpha, t_{\chi,LSR})$ are two dotted double sided arrows that are used to describe real arcs in Fig. 3. We define $\bar{\chi}$ as the reverse direction of χ, i.e., if χ is direction $\boldsymbol{n}$ (respectively, $\boldsymbol{e}$, $\boldsymbol{s}$, and $\boldsymbol{w}$), $\bar{\chi}$ represents $\boldsymbol{s}$ (respectively, $\boldsymbol{w}$, $\boldsymbol{n}$, and $\boldsymbol{e}$). Now we discuss four emergency strategies as follows:

1) The straight traffic flow from direction χ needs to be forbidden. It is realized by keeping the traffic light GS_χ off. In the TPN model, a token is deposited in $p_{\chi,S}$. Then $b^i_{\chi,S}$ obtains a token meaning that the straight ban signal light is turning on. There are two situations that the emergency strategy is realized:

- $p_{\chi 4}$ contains a token which means GS_χ is on. Then the immediate transition $t_{\chi,S2}$ is enabled and fires such that a token is transferred from $p_{\chi 4}$ to $p_{\chi 6}$. Hence, GS_χ is immediately turned off and YR_χ is turned on.
- $p_{\chi 4}$ contains no token which means GS_χ is off at the moment. $t_{\chi 5}$ is prevented from firing because of the inhibitor arc linked from $p_{\chi,S}$ with a token. When $p_{\chi 8}$ gets a token, $t_{\chi,S1}$ is enabled and fires such that the token is transferred from $p_{\chi 8}$ to $p_{\chi 10}$. Hence, GS_χ remains off.

Notice that we use $t_{\chi 2}$ to realize the synchronization of lights GS_χ and GR_χ. Under this strategy, a token stays in $p_{\chi 10}$ until $t_{\chi 10}$ fires, i.e., the time duration ofGR_χ is reached.

2) The right-turning traffic flow from direction χ should be stopped. It is realized by keeping the traffic light GR_χ off. In the TPN model, a token is deposited in $p_{\chi,R}$. Then $b^i_{\chi,R}$ obtains a token meaning that the right ban signal light is turning on. There are two situations that the emergency strategy is realized:

- $p_{\chi 5}$ contains a token which means GR_χ is on. Then the immediate transition $t_{\chi,R2}$ is enabled and fires such that a token is transferred from $p_{\chi 5}$ to $p_{\chi 7}$. Hence, the traffic light is immediately turned from GR_χ to YR_χ.
- $p_{\chi 5}$ contains no token which means GR_χ is off at the moment. $t_{\chi 6}$ is not enabled because of the inhibitor arc linked from $p_{\chi,R}$ with a token. When $p_{\chi 9}$ gets a token, $t_{\chi,R1}$ is enabled and fires such that the token is transferred from $p_{\chi 7}$ to $p_{\chi 11}$. Hence, GR_χ remains off.

3) The left-turning traffic flow from direction χ should be stopped. It is realized by keeping the traffic light GL_χ off. In the TPN model, a token is deposited in $p_{\chi,L}$. Then $b^i_{\chi,L}$ obtains a token meaning that the left ban signal light is turning on. There are two situations that the emergency strategy is realized:

- $p_{\chi 3}$ contains a token which means GL_χ is on. Then the immediate transition $t_{\chi,L2}$ is enabled and fires such that a token is transferred from $p_{\chi 3}$ to $p_{\chi 2}$. Hence, GL_χ is immediately turned off and YL_χ is turned on. In this situation, both $t_{\chi 2}$ and $t_{\chi 3}$ do not fire.
- $p_{\chi 3}$ contains no token which means GL_χ is off at the moment. $t_{\chi 2}$ is not enabled because of the inhibitor arc linked from $p_{\chi,L}$ with a token. When both $p_{\chi 10}$ and $p_{\chi 11}$ get their tokens, $t_{\chi,L1}$ is enabled and fires such that the token is transferred from $p_{\chi 10}$ and $p_{\chi 11}$ to $p_{\chi 1}$. Hence, GL_χ remains off.

In the operation of the traffic-light control model in Fig. 3, during a traffic light transition cycle, a token is deposited into or removed from p_β at direction χ. When GL_χ is changed to YL_χ, i.e., $t_{\chi 3}$ fires and a token is filled into or removed from p_β. In the emergency one, however, $t_{\chi 3}$ will not fire. Thus dotted double sided arrows $(p_\beta, t_{\chi,L1})$ and $(p_\beta, t_{\chi,L2})$ are drawn in order to preserve the token count in p_β.

4) If there exists a token in $p_{\chi,LSR}$, all traffic flows from direction χ should be forbidden. It is realized by keeping all traffic lights GS_χ, GR_χ, and GL_χ off. In the TPN model, a token is deposited in $p_{\chi,LSR}$. At this situation, each of $p_{\chi,R}$, $p_{\chi,S}$, and $p_{\chi,L}$ contains a token. Then each of $b^i_{\chi,R}$, $b^i_{\chi,S}$ and $b^i_{\chi,L}$ gets a token meaning that all ban signal lights are turning on. There are two situations that the emergency strategy is realized:

- $p_{\chi 1}$ contains a token which means R_χ is on, and $t_{\chi 1}$ is prevented from firing because of the inhibitor arc from $p_{\chi,LSR}$. At this situation, $t_{\chi,LSR}$ fires and a token is deposited into or removed from p_α and p_β. Note that both p_α and p_β are marked or neither is. Hence, R_χ is kept on.
- $p_{\chi 1}$ contains no token, due to the tokens in $p_{\chi,S}$, $p_{\chi,R}$ and $p_{\chi,L}$ such that the traffic lights can be turned from green ones to yellow ones, and then to red ones. Thus R_χ is turned on and will be kept on.

Note that, in the strategy, neither of $t_{\chi 1}$ and $t_{\chi 3}$ will fire. The dotted double sided arrows are drawn to preserve the token count in p_α and p_β.

When tokens in $p_{\chi,R}$, $p_{\chi,S}$, and $p_{\chi,L}$ are removed, $b^i_{\chi,R}$, $b^i_{\chi,S}$ and $b^i_{\chi,L}$ will not contain any token either. At this situation all ban signal lights are turned off and traffic lights return to their normal strategies from the emergency ones. We will discuss that in detail via reachability graph analysis.

C. Level-II Strategy

Level-II emergency traffic light control strategy adopting warning signal lights is designed via a TPN as shown in Fig. 9. If there respectively exists a token in $p_{\chi,S'}$, $p_{\chi,R'}$, and $p_{\chi,L'}$, the traffic flow from direction χ should obtain a warning signal

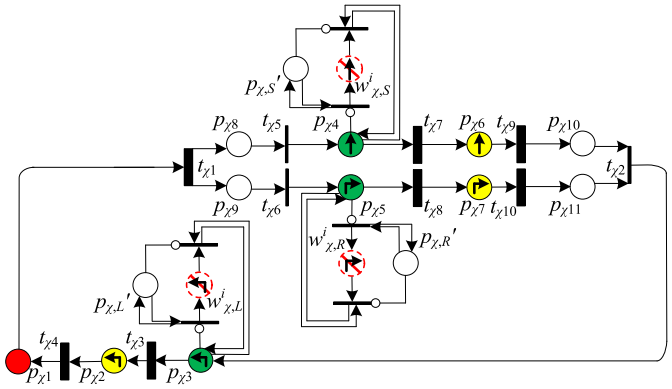

Fig. 9. The TPN model of strategy II.

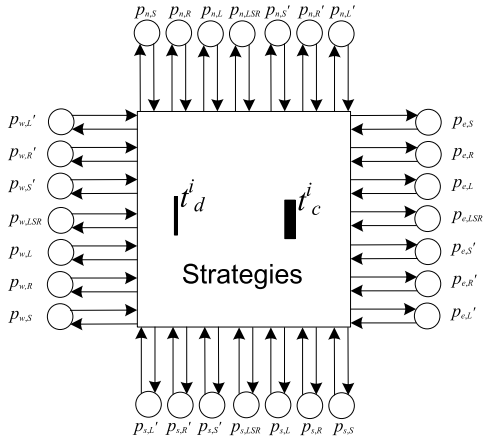

Fig. 10. The dynamic TPN model of a traffic light strategy decision.

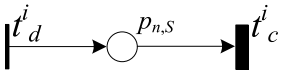

Fig. 11. A dynamic TPN model of traffic light strategy decision.

for vehicles not to run straightly, turn right, and turn left, respectively. When there is no token in $p_{\chi 3}$, $p_{\chi 4}$, or $p_{\chi 5}$, a token will be generated in $w^i_{\chi,L}$, $w^i_{\chi,S}$, or $w^i_{\chi,R}$, respectively, which means that left, straight, or right warning signal light is turned on when the left, straight, or right traffic light is off. At this situation, vehicles could change their directions by following the warning signals. Note that more than one but not all of $p_{\chi,S}{}'$, $p_{\chi,R}{}'$ and $p_{\chi,L}{}'$ can contain a token.

D. Strategies to Prevent Traffic Congestion

Now a TPN model of the traffic light strategy is designed in Fig. 10. Given the traffic flow condition, strategies (when and where to operate the ban lights and warning ones) should be obtained. Here we adopt certain strategies to decide the arcs to be added to connect $p_{\chi,S}$, $p_{\chi,R}$, $p_{\chi,L}$, $p_{\chi,LSR}$, $p_{\chi,S}{}'$, $p_{\chi,R}{}'$, and $p_{\chi,L}{}'$ with transitions t^i_d and t^i_c. If a token needs to be deposited in $p \in \{p_{\chi,S}, p_{\chi,R}, p_{\chi,L}, p_{\chi,LSR}\}$, two arcs (t^i_d, p) and (t^i_c, p) are drawn. Note that the detailed emergency strategies are determined by the position of the incident which will be presented in the following section.

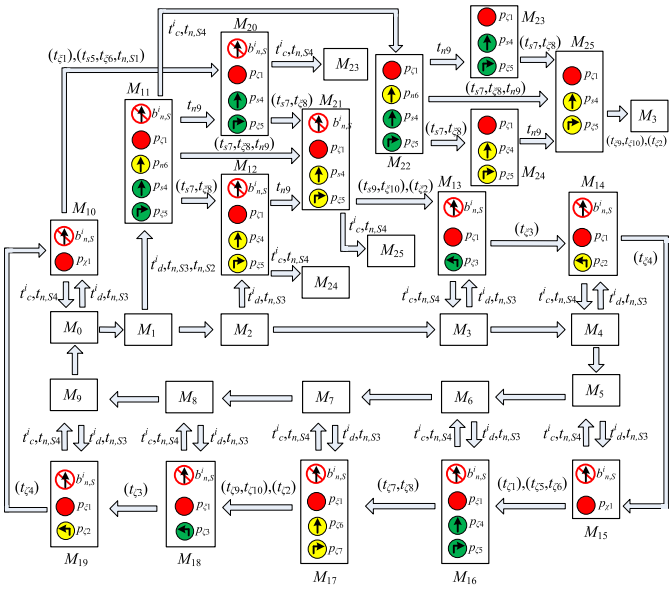

Fig. 12. The reachability graph of the emergency strategy of Fig. 8 under the condition of Fig. 11.

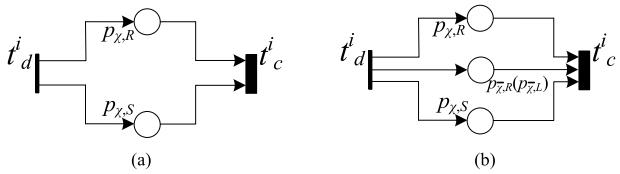

Fig. 13. Two dynamic TPN models of traffic light strategy decision.

E. Property Analysis

When a TPN model is built, We can verify the correctness of the TPN-based traffic light strategy by using a reachability graph analysis method. Here a reachability graph is constructed with each arc corresponding to a sequence of transitions containing only one timed one. Besides, these transitions that fire at the same time are put in parentheses. This way allows us to reduce the size of the graph greatly. The reachability analysis can also be done through a tool such as TimeNet [44].

We now give an emergency strategy as an example. Suppose that the straight traffic flow from the North direction needs to be forbidden while others go under their normal way. The TPN model of such strategy generated from the model in Fig. 10 is built as shown in Fig. 11, where there is only one input place of t^i_c and output place of t^i_d, i.e., $p_{n,S}$. Under such situation, we can obtain the reachability graph of the model in Fig. 8 as shown in Fig. 12. Since this graph is a finite circle containing 26 markings $M_0 - M_{25}$ corresponding to 26 traffic light states that are to ensure the traffic flow control, the TPN model is reversible. Similarly, we can verify the correctness of the other strategies by deriving their reachability graph.

By using reachability graph analysis, we find some situations where conflicting traffic flows appear. There are two situations: both the straight and right traffic flows from direction χ need to be forbidden as shown in Fig. 13 (a), and the straight

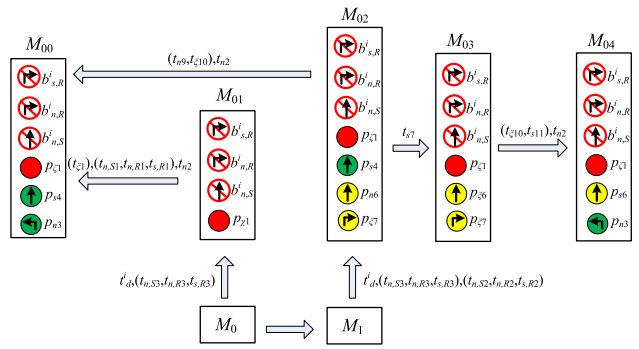

Fig. 14. The reachablity graph under strategy Fig. 13 (b).

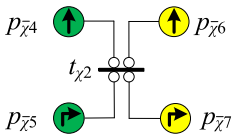

Fig. 15. A synchronization model.

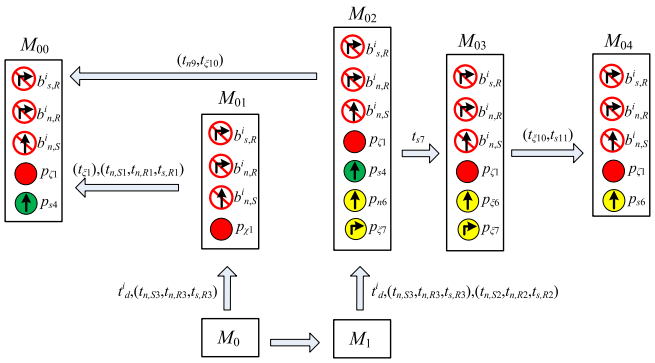

Fig. 16. A part of reachability graph of the emergency strategy of Fig. 8 under the condition of Fig. 13 (b).

and right traffic flows frwom direction χ and the right (or left) traffic flow from direction $\bar{\chi}$ need to be forbidden while others go under their normal way as shown in Fig. 13(b). We take Fig. 13(b) as an example and construct its reachability graph. In the graph there is a state M_{00} as shown in Fig. 14 where GS_s and GL_n are on at the same time. Permitted by such strategy, traffic flows from south driving straight and from north turning left have a conflict. Also at M_{04} we have a conflict. To solve this problem, we need to ensure the proper synchronization of $t_{\chi 2}$ and $t_{\bar{\chi}2}$ and we construct a model in Fig. 15. As a result, the reachability graph is constructed as shown in Fig. 16.

Suppose that the traffic flows from all directions should be forbidden, i.e., the state of the signal should be $M_0 = (R_n, R_e, R_s, R_w)$. We should adopt the strategy in Fig. 17. In the TPN model as shown in Fig. 8, a transition firing sequence $\sigma = (t_{\xi,LSR}),(t_{\zeta,LSR})$, can fire repeatedly where $M_0[\sigma > M_0$ as shown in Fig. 18. It is a livelock and has no benefit to traffic control. A recovery model is built in Fig. 19. If all $p_{\chi 1}$ and $p_{\chi,LSR}$ contain tokens, transition t_{ML} fires and a token is generated in p_{ML}. Transitions $t_{n,LSR}$, $t_{s,LSR}$, $t_{e,LSR}$, and $t_{w,LSR}$ cannot fire because of the inhibitor arcs from p_{ML}.

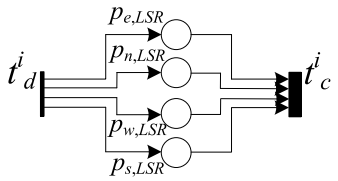

Fig. 17. A dynamic TPN model of traffic light strategy decision.

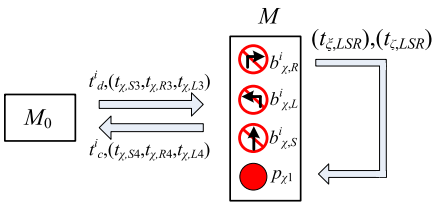

Fig. 18. A part of reachability graph of the emergency strategy of Fig. 8 under the condition of Fig. 17.

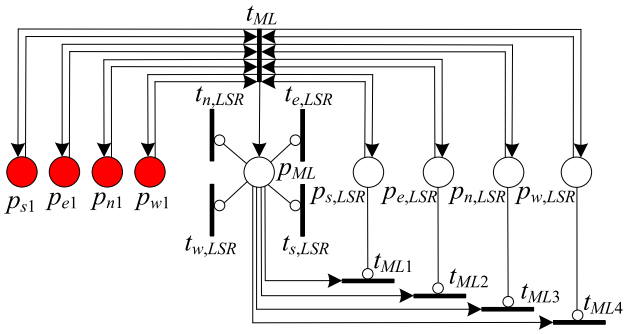

Fig. 19. A livelock prevention model.

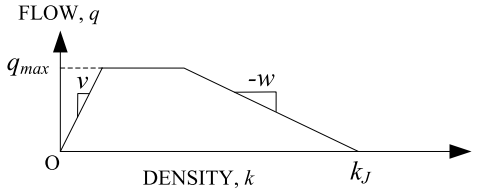

Fig. 20. Flow-density relationship for the generalized CTM [22].

Thus σ is prevented. When the emergency strategy stops, tokens in $p_{\chi,LSR}$ are removed. Then one of $t_{ML1} - t_{ML4}$ fires by removing the token in p_{ML}, and the traffic lights return to operate under their normal strategy.

Notice that other strategies can be obtained and verified in a similar way when the straight, left, or right traffic flow from one of the four directions needs to be forbidden while others go under their normal way. Thus the correctness of the TPN model in Fig. 8 is verified. By using the reachability graph analysis method we can verify the correctness of the TPN model in Fig. 9 as well.

IV. Case Study

We have designed emergency traffic light strategies by using a TPN model and verified that such strategies can be correctly implemented with co-design of hardware and software. Now we evaluate the effectiveness of the proposed strategy by

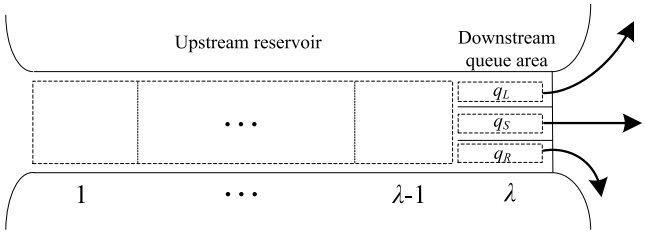

Fig. 21. Link a in two-way grid networks.

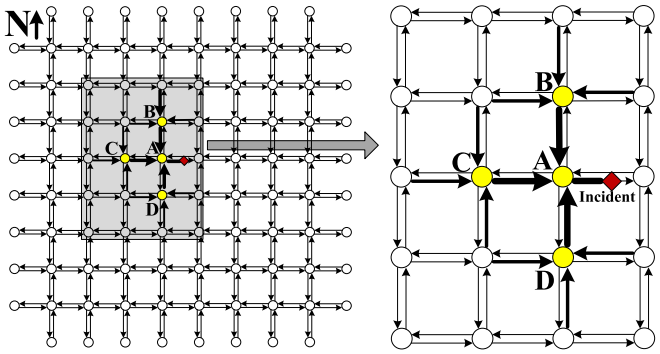

Fig. 22. An 8×8 two-way grid network.

employing MATLAB software through simulation. First we build a two-way rectangular grid network based on a cell transmission model (CTM) [45], [46]. Then we extend the model in [47] by considering the vehicle route-changing rate and traffic signal strategies. Through the simulation of our designed model, we identify the influences of some important parameters, i.e., route-changing behaviors of drivers, the time to operate the emergency strategy, and the inflow of the traffic network, on the traffic congestion formation and dissipation.

A. Cell Transmission Model

Daganzo [45], [46] proposes CTM to simplify the solution scheme of the Lighthill-Whitham-Richards (LWR) model [48], [49] by adopting the following relationship between traffic flow q (vehicles per hour) and density k (vehicles per lane-mile) as shown in Fig. 20:

$$q = \min\{vk, q_{\max}, w(k_J - k)\}, \quad 0 \le k \le k_J$$

where v (miles per hour) is the free flow speed and w (miles per hour) is the speed of all backward moving waves, and $q_{\max}$ and k_J denote the inflow capacity (or maximum allowable inflow) and jam density, respectively. We have the following CTM:

$$y_i(t) = \min\{n_{i-1}(t, Q_i(t), w(N_i(t) - n_i(t))/v\}$$
$$n_i(t+1) = n_i(t) + y_i(t) - y_{i+1}(t)$$

where $y_i(t)$ is the number of vehicles that flow into cell i during time interval t, $n_i(t)$ is the number of vehicles in cell i before t, $N_i(t)$ denotes the maximum number of vehicles that can be contained in cell i during t, and $Q_i(t)$ denotes the inflow capacity in cell i during t.

TABLE II
SYMBOLS AND THEIR MEANINGS

Symbols	Meaning
$n^i_a(t)$	The number of vehicles contained in cell i of link a at the start of time interval t
$n^i_{ab}(t)$	The number of vehicles contained in cell i of link a and take link b as the next link at the start of time interval t
$y^i_a(t)$	The number of vehicles that flow into cell i of link a in time interval t
$y^i_{ab}(t)$	The number of vehicles that flow into cell i of link a and take link b as the next link in time interval t
$Q^i_a(t)$	The maximum number of vehicles that can flow into cell i of link a in time interval t
$N^i_a(t)$	The maximum number of vehicles that can be present in cell i of link a in time interval t
ϕ_{ab}	Proportion of vehicles traveling from link a to link b
α_{ab}	Proportion of stopline width devoted to vehicles traveling from link a to link b
$d^i_a(t)$	The sum of the congestion delay of vehicles contained in cell i of link a at time interval t
$d(t)$	The total congestion delay of vehicles contained in the whole network at time interval t

B. A Traffic Network and Its CTM

In the networks as shown in Fig. 21, each link a is divided into two distinct zones: downstream queue storage areas q_L, q_S and q_R where vehicles are organized into separate turning movements (left in q_L, straight in q_S, and right in q_R), and an upstream reservoir where the turning movements are mixed. We assume that the upstream reservoir is composed of λ cells, and the length of the channelized queue area is short and equals the length of a cell ($\lambda + 1$). Note that the length of the channelized downstream queue area is set to one cell because of the results in [47] that the congestion time is reduced when the channelized downstream queue area is very short. As shown in Fig. 22, we construct an 8×8 two-way grid network to test the model. All boundary nodes are both origins and destinations. φ_L, φ_S, and φ_R denote, respectively, the proportions of vehicles travelling in the left turning direction, in the ahead direction and in the right turning direction. Stop line width assignment variables α_L, α_S, α_R denote, respectively, the proportions of the segregated queue areas devoted to the left turning queue storage area, to the ahead queue storage area and to the right turning queue storage area. According to the definition, we have $\varphi_L + \varphi_S + \varphi_R = 1$ and $\alpha_L + \alpha_S + \alpha_R = 1$. We adopt a 'balanced' layout of stop line assignment [1] such that the stop line widths devoted to the ahead direction and to the turning direction are in exactly the same ratio as the demands, i.e., $\varphi_L = \alpha_L$, $\varphi_S = \alpha_S$, and $\varphi_R = \alpha_R$.

Table II describes the symbols used in the following content. Note that traffic rules will not be changed and the vehicles in the downstream queue areas will not change lanes. Using the network model, we design a network traffic simulation model based on the time-step method. The inflow formulation can be classified into three categories: inflow of upstream reservoir ($i = 1$), inflow of upstream cells ($1 < i \le \lambda - 1$), and inflow of channelized downstream queue area ($i = \lambda$). We consider the influence of traffic flow lane changing

behavior to illustrate the designed traffic light strategy. The inflow formulation is presented as follows:

1) Inflow of upstream cells

The inflow of upstream cells can be calculated by:

$$y_a^i(t) = \min\{n_a^{i-1}(t), Q(t), w(N - n_a^i(t))/v\}, \quad 1 < i \le \lambda - 1 \tag{1}$$

$$y_{ab}^i(t) = \varphi_{ab} y_a^i(t), \quad 1 < i \le \lambda - 1 \tag{2}$$

2) Inflow of the channelized downstream queue area

The up bound of inflow of the downstream queues area for vehicles travelling from link a to link b is computed as follows:

$$y'_{ab}(t) = \min\{\alpha_{ab} Q(t), w(\alpha_{ab} N - n_{ab}^{\lambda}(t))/v\} \tag{3}$$

Let b_l and b_m be respectively a set of links leading to and leaving link b. Because of interference between turning vehicles and ahead vehicles [1], the total inflow of the channelized queues area can be formulated as follows

$$y_a^{\lambda}(t) = \min_{b \in b_m}\{y'_{ab}(t)/\alpha_{ab}\} \tag{4}$$

The inflow of each direction can be calculated as follows

$$y_{ab}^{\lambda}(t) = \min\{\varphi_{ab} y_a^{\lambda}(t), \alpha_{ab} n_a^{\lambda-1}(t)\} \tag{5}$$

We model the proposed traffic light strategy in the CTM model. We suppose that in our proposed two-level strategy, in each direction, there is at most one warning light or ban light being on. We suppose that when seeing a ban signal at the direction where vehicles intend to drive, d_1 percent of them change their routes, while seeing a warning signal, d_2 percent do so. Thus we have the proportion of traffic flow in the segregated queue area computed as follows. When a warning light at direction b is on and the other two directions are supposed to be c and d. Let φ'_{ab} denote the proportion of vehicles traveling from link a to link b. At a ban or warning light-on situation, we have

$$\begin{aligned} &\varphi'_{ab} = \varphi_{ab}(1 - d_i), \quad \varphi'_{ac} = \varphi_{ac} + \varphi_{ab} d_i/2, \text{and} \\ &\varphi'_{ad} = \varphi_{ad} + \varphi_{ab} d_i/2 \end{aligned} \tag{6}$$

where i =1 if the light is a ban light and i =2 if it is a warning light.

If such lights are on at direction b', the total inflow of the channelized queues area can be obtained via (3)-(5), where $\varphi_{ab} = \varphi'_{ab}$ is computed by (6).

3) Inflow of upstream reservoir and outflow of the channelized downstream queue area.

$y^{\lambda+1}$ is defined as the outflow of the terminal cells.

$$y_{ab}^{\lambda+1}(t) = \min\{n_{ab}^{\lambda}(t), \alpha_{ab} Q^{\lambda}(t), w(N - n_b^1(t))/v\} \tag{7}$$

$$y_a^1(t) = \Sigma_{b \in b_l} y_{ba}^{\lambda+1}(t) \tag{8}$$

$$y_a^{\lambda+1}(t) = \Sigma_{b \in b_m} y_{ab}^{\lambda+1}(t) \tag{9}$$

The update of the number of vehicles contained in each cell, is formulated as follows

$$n_a^i(t+1) = n_a^i(t) + y_a^i(t) - y_a^{i+1}(t), \quad 1 \le i \le \lambda \tag{10}$$

Traffic signal control and incidents are modeled by modifying the value of the corresponding flow capacity of the affected cells. $Q_{ab}^{\lambda}(t) = 0$ if t belongs to the period when the red traffic light is on. At this time, vehicles running to link b in cell λ of link a are forbidden. $Q_a^i(t) = 0$ if t belongs to the period with an obstruction on cell i. We assume that $Q_a^i(t)$ and $N_a^i(t)$ are independent of cell number and time, i.e., $Q_a^i(t) = Q$ and $N_a^i(t) = N$.

TABLE III

PARAMETERS FOR THE CTM [47]

Parameters	*Values*
The length of each time interval	5 s
Jam density	133 vehicles/km/lane (i.e., 7.5 m for every vehicle in each lane)
Free-flow speed	54 km/h (i.e., 15 m/s), and backward shock-wave speed: 21.6 km/h (i.e., 6 m/s)
Number of lanes	2
Flow capacity	1800 vehicles/h/lane (i.e., 2.5 vehicles/time interval/cell)
Cell length	75 m, and the holding capacity of each cell is 20 vehicles.
The number of cells of each link	9 (i.e., the length of every link is 675m)

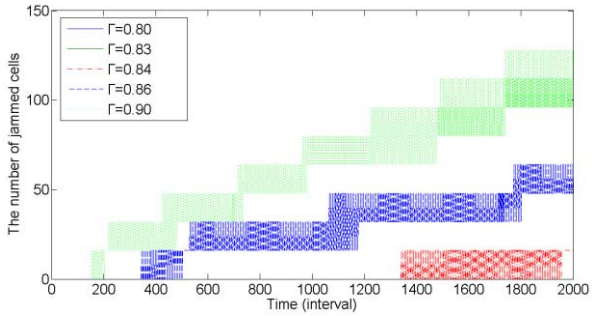

Fig. 23. Congestion formulation when Γ =0.80, 0.83, 0.84, 0.86, and 0.90.

Traffic jam size is used to describe the effect of congestion. A cell is called a jammed one if its density in the upstream reservoir or in any direction of the downstream channelized area is greater than $0.9N$ [47]. The size of traffic jams is described in terms of the total number of jammed cells.

The analysis period of interest is divided into 2000 intervals (i.e., 2.78 h). The traffic demand is Γ vehicles per interval for each origin. Define δ as the ratio that the green signal time divides the traffic light cycle time. We have a property as follows.

Property 1: Congestion appears if $\Gamma > \delta Q$.

Note that during a cycle T, the whole amount of traffic riding in a lane and intending to driving left from the original is $\Gamma * T * \alpha_L$ while according to formula (7) the outflow from the lane is less that $\delta * T * Q * \alpha_L$. If $\Gamma > \delta Q$, the inflow overweight the outflow and the downstream queue storage area q_L will finally be blocked. The blockage of q_L will lead to the congestion of the whole road.

CTM parameters are taken from [47] as shown in Table III. The flow proportions for all directions are: $\varphi_L = 0.2$, $\varphi_S = 0.5$, and $\varphi_R = 0.3$. The initial network is empty, and some time intervals are required to allow the system to stabilize. We suppose that the traffic inflow and outflow of the original points are restricted by the same traffic light

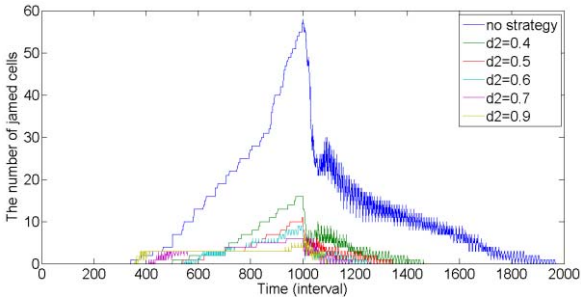

Fig. 24. Congestion formulation and dissipation under no strategy and emergency ones such that the strategy begins from 301st interval to 1000th interval and d_1 =0.9, and d_2 =0.4, 0.5, 0.6, 0.7 and 0.9.

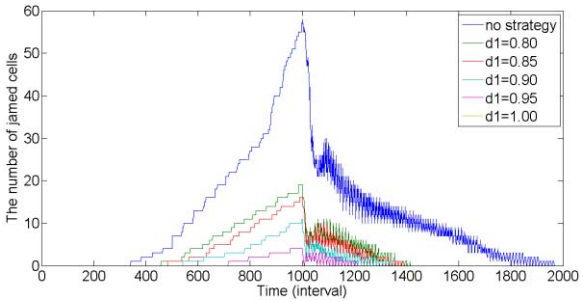

Fig. 25. Congestion formulation and dissipation under no strategy and emergency ones such that the strategy begins from 301st interval to 1000th interval and d_1 =0.80, 0.85, 0.90, 0.95 and 1.00 , and d_2 =0.5.

signal as well as the traffic light time duration as described in Fig. 3. We evaluate the impact of factor Γ on traffic congestion as shown in Fig. 23 which demonstrates Property 1, i.e., if $\Gamma < \delta Q \approx 0.833$, e.g. $\Gamma = 0.80$ and 0.83, there is no congestion.

We install a single incident in our simulation: a single incident occurs at the 5th cell of a link in the network as shown in Fig. 22. We construct emergency strategies: the ban signal strategy works at intersection A while the warning signal strategies work at intersections B, C and D. In detail, a dynamic TPN model in Fig. 10 can be constructed to execute the strategies: there are arcs from t_d^A to $p_{n,l}$, $p_{w,S}$, and $p_{s,R}$ (also denoted by $p_{n,L}^A$, $p_{w,S}^A$, and $p_{s,R}^A$), and from these places to t_c^A. Tokens are filled in $p_{n,L}^A$, $p_{w,S}^A$, and $p_{s,R}^A$. Similarly, arcs are added from t_d^B to $p_{e,L'}^B$, $p_{n,S'}^B$, and $p_{w,R'}^B$ and from these places to t_c^B; from t_d^C to $p_{n,L'}^C$, $p_{w,S'}^C$, and $p_{s,R'}^C$ and from these places to t_c^C; and from t_d^D to $p_{w,L'}^D$, $p_{s,S'}^D$, and $p_{e,R'}^D$ and from these places to t_c^D.

C. Simulation Results

First, we study the effect of the driving route changing rate d_1 and d_2 on jam formation and dissipation. The incident occurs at the 301st interval and is cleared at the 1000th interval where the traffic demand is set to be $\Gamma = 0.5$. Simulation results of congestion formulation and dissipation are shown in Figs. 24-25. We can learn that under no strategy at this traffic situation, congestion begins at the 341th time interval; the maximum jammed cell count is 58 at the 1,000th time interval; and the congestion dissipation takes in total 1966 time

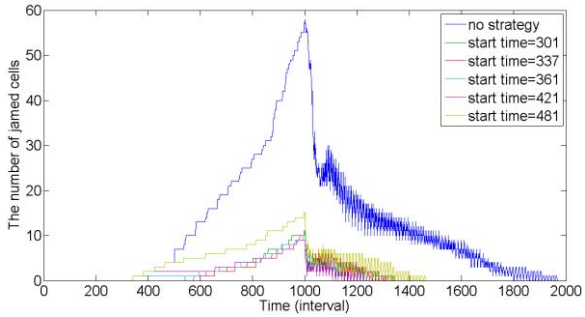

Fig. 26. Congestion formulation and dissipation under no strategy and emergency ones such that the strategy begins from 301st, 337th, 361st, 421st, and 481st intervals, respectively, to 1000th interval and $d_1 = 0.9$, and $d_2 = 0.5$.

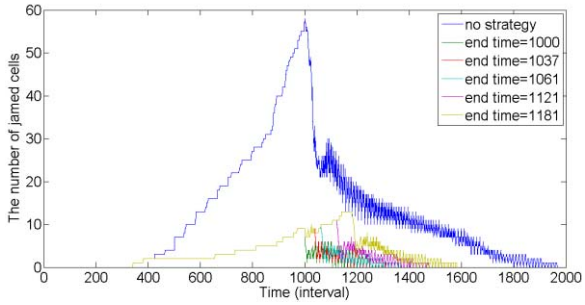

Fig. 27. Congestion formulation and dissipation under no strategy and emergency ones such that the strategy begins from 421st interval to 1000th, 1037th, 1061st, 1121st, and 1181st intervals, respectively, and $d_1 = 0.9$, and $d_2 = 0.5$.

intervals. Fig. 24 also shows the results under the proposed strategy where it begins from 301st interval to 1000th interval in cases of $d_1 = 0.9$, and $d_2 = 0.4$, 0.5, 0.6, 0.7 and 0.9. The maximum jammed cell count is no more than 10 if the turning rate d_2 is not less than 0.5. At this situation, less than 350 time intervals are needed to completely dissipate the congestion. Fig. 25 shows the results when $d_2 = 0.5$ but d_1 changes, i.e., 0.80, 0.85, 0.90, 0.95 and 1.00. We can learn that the maximum jammed cell count is no more than 10 if $d_1 \geq 0.9$. If $d_1 \geq 0.98$, there is no congestion at all.

Second, we study the effect of the start time to adopt the emergency strategy. Under all emergency strategies, the time needed for the dissipation is much less than the self-evolved traffic. We obtain the result from Fig. 26 that under the constant inflow $\Gamma = 0.5$, the turning rates $d_1 \geq 0.9$ and $d_2 \geq 0.5$. If the reaction time towards the incident is less than 10 minutes (i.e., at the 421st time interval), the maximum jammed cell count is no more than 10 and less than 350 time intervals are needed to completely dissipate the congestion. Thus the emergency strategy indeed offers excellent performance.

Third, we study the effect of the time to stop the emergency strategy that begins from the 421st interval. From Fig. 27 we can see that the congestion starts to dissipate at the stop of the emergency strategy. For example, if the end time of the strategy is 10 minutes after the clearance of the incident (i.e. at the 1121st time interval), the maximum jammed cell count is 12 and more than 600 time intervals are needed to completely

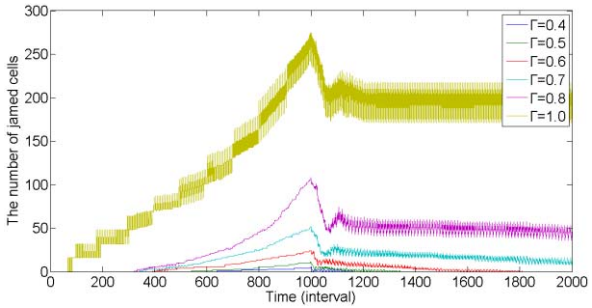

Fig. 28. Congestion formulation when $\Gamma = 0.4, 0.5, 0.6, 0.7, 0.8$, and 1.0 and the strategy begins from 301st interval to 1000th interval and $d_1 = 0.9$, and $d_2 = 0.5$.

dissipate the congestion. Thus the emergency strategy should be stopped as soon as possible when the incident is cleared because the ban signal strategy causes congestion as well.

Finally, we evaluate the impact of factor Γ as shown in Fig. 28 when the strategy begins from the 301st interval to 1000th interval and d_1 =0.9, and d_2 =0.5. We can see that if $\Gamma \leq$0.6, the emergency strategy can be accepted. If not, it causes congestion and takes more than 800 time intervals to dissipate.

In conclusion, the emergency strategies can be adopted to deliver highly desired performance under the following conditions that the constant inflow $\Gamma \leq 0.5$, the turning rates $d_1 \geq 0.9$ and $d_2 \geq 0.5$ and the incident reaction time is no more than 10 minutes.

V. Conclusions

This work designs a traffic-light control system at a signalized intersection to prevent large-scale traffic congestion caused by incidents. Normal and emergency traffic light control strategies are formulated. Their control logic is presented in detail and proved to be valid by using timed Petri nets. This work verifies the effectiveness of the strategy through a simulation study where an extended CTM model is used to construct the traffic network. The strategies perform well in response to an incident under certain conditions including timely termination of their use after the clearance of the incident. The results can be used to improve the state of the art in preventing urban road traffic congestion caused by incidents. Future work intends to study the applications of the proposed strategies in other complicated traffic networks.

References

[1] C. Wright and P. Roberg, "The conceptual structure of traffic jams," *Transp. Policy*, vol. 5, no. 1, pp. 23–35, 1998.

[2] H. Al-Deek, T. W. P. Lochrane, C. V. S. R. Chandra, and A. Khattak, "Diversion during unexpected congestion on toll roads: The role of traffic information displayed on dynamic message signs," *IET Intell. Transp. Syst.*, vol. 6, no. 2, pp. 97–106, Jun. 2012.

[3] V. Milanes, J. Godoy, J. Villagra, and J. Perez, "Automated on-ramp merging system for congested traffic situations," *IEEE Trans. Intell. Transp. Syst.*, vol. 12, no. 2, pp. 500–508, Jun. 2011.

[4] P. Zhang, C.-X. Wu, and S. C. Wong, "A semi-discrete model and its approach to a solution for a wide moving jam in traffic flow," *Phys. A, Statist. Mech. Appl.*, vol. 391, no. 3, pp. 456–463, 2012.

[5] R. Bauza and J. Gozalvez, "Traffic congestion detection in large-scale scenarios using vehicle-to-vehicle communications," *J. Netw. Comput. Appl.*, vol. 36, no. 5, pp. 1295–1307, 2013.

[6] F. Knorr, D. Baselt, M. Schreckenberg, and M. Mauve, "Reducing traffic jams via VANETs," *IEEE Trans. Veh. Technol.*, vol. 61, no. 8, pp. 3490–3498, Oct. 2012.

[7] F. Terroso-Saenz, M. Valdes-Vela, C. Sotomayor-Martinez, R. Toledo-Moreo, and A. F. Gomez-Skarmeta, "A cooperative approach to traffic congestion detection with complex event processing and VANET," *IEEE Trans. Intell. Transp. Syst.*, vol. 13, no. 2, pp. 914–929, Jun. 2012.

[8] M. Papageorgiou, C. Diakaki, V. Dinopoulou, A. Kotsialos, and Y. Wang, "Review of road traffic control strategies," *Proc. IEEE*, vol. 91, no. 12, pp. 2043–2067, Dec. 2003.

[9] D. I. Robertson and R. D. Bretherton, "Optimizing networks of traffic signals in real time—The SCOOT method," *IEEE Trans. Veh. Technol.*, vol. 40, no. 1, pp. 11–15, Feb. 1991.

[10] P. R. Lowrie, *SCATS: A Traffic Responsive Method of Controlling Urban Traffic Control*. New South Wales, Australia: Roads and Traffic Authority, 1992.

[11] M. Dotoli, M. P. Fanti, and C. Meloni, "A signal timing plan formulation for urban traffic control," *Control Eng. Pract.*, vol. 14, no. 11, pp. 1297–1311, Nov. 2006.

[12] S. F. Cheng, M. A. Epelman, and R. L. Smith, "CoSIGN: A parallel algorithm for coordinated traffic signal control," *IEEE Trans. Intell. Transp. Syst.*, vol. 7, no. 4, pp. 551–564, Dec. 2006.

[13] B. D. Schutter and B. D. Moor, "Optimal traffic light control for a single intersection," *Eur. J. Control*, vol. 4, no. 3, pp. 260–276, 1998.

[14] K. Aboudolas, M. Papageorgiou, and E. Kosmatopoulos, "Store-and-forward based methods for the signal control problem in large-scale congested urban road networks," *Transp. Res. C, Emerg. Technol.*, vol. 17, no. 2, pp. 163–174, Apr. 2009.

[15] K. Aboudolas, M. Papageorgiou, A. Kouvelas, and E. Kosmatopoulos, "A rolling-horizon quadratic-programming approach to the signal control problem in large-scale congested urban road networks," *Transp. Res. C, Emerg. Technol.*, vol. 18, no. 5, pp. 680–694, Apr. 2010.

[16] A. Kouvelas, K. Aboudolas, M. Papageorgiou, and E. B. Kosmatopoulos, "A hybrid strategy for real-time traffic signal control of urban road networks," *IEEE Trans. Intell. Transp. Syst.*, vol. 12, no. 3, pp. 884–894, Sep. 2011.

[17] S. Zhao, Y. Chen, and J. A. Farrell, "High-precision vehicle navigation in urban environments using an MEM's IMU and single-frequency GPS receiver," *IEEE Trans. Intell. Transp. Syst.*, vol. 17, no. 10, pp. 2854–2867, Oct. 2016.

[18] N. Geroliminis, J. Haddad, and M. Ramezani, "Optimal perimeter control for two urban regions with macroscopic fundamental diagrams: A model predictive approach," *IEEE Trans. Intell. Transp. Syst.*, vol. 14, no. 1, pp. 348–359, Mar. 2013.

[19] M. Ramezani, J. Haddad, and N. Geroliminis, "Dynamics of heterogeneity in urban networks: Aggregated traffic modeling and hierarchical control," *Transp. Res. B, Methodol.*, vol. 74, pp. 1–19, Apr. 2015.

[20] J. Haddad, M. Ramezani, and N. Geroliminis, "Cooperative traffic control of a mixed network with two urban regions and a freeway," *Transp. Res. B, Methodol.*, vol. 54, no. 8, pp. 17–36, Aug. 2013.

[21] Y. Ji and N. Geroliminis, "On the spatial partitioning of urban transportation networks," *Transp. Res. B, Methodol.*, vol. 46, no. 10, pp. 1639–1656, Dec. 2012.

[22] J. Haddad and N. Geroliminis, "On the stability of traffic perimeter control in two-region urban cities," *Transp. Res. B, Methodol.*, vol. 46, no. 9, pp. 1159–1176, Nov. 2012.

[23] P. Roberg, "Distributed strategy for eliminating incident-based traffic jams from urban networks," *Traffic Eng. Control*, vol. 36, no. 6, pp. 348–354, 1995.

[24] J. Long, Z. Gao, P. Orenstein, and H. Ren, "Control strategies for dispersing incident-based traffic jams in two-way grid networks," *IEEE Trans. Intell. Transp. Syst.*, vol. 13, no. 2, pp. 469–481, Jun. 2012.

[25] M. C. Zhou and F. DiCesare, *Petri Net Synthesis for Discrete Event Control of Manufacturing Systems*. Norwell, MA, USA: Kluwer, 1993.

[26] M. C. Zhou and K. Venkatesh, *Modeling, Simulation, and Control of Flexible Manufacturing Systems: A Petri Net Approach*. Singapore: World Scientific, 1998.

[27] K. M. Ng, M. B. I. Reaz, and M. A. M. Ali, "A review on the applications of Petri nets in modeling, analysis, and control of urban traffic," *IEEE Trans. Intell. Transp. Syst.*, vol. 14, no. 2, pp. 858–870, Jun. 2013.

[28] G. F. List and M. Cetin, "Modeling traffic signal control using Petri nets," *IEEE Trans. Intell. Transp. Syst.*, vol. 5, no. 3, pp. 177–187, Sep. 2004.

[29] Y.-S. Huang and T.-H. Chung, "Modeling and analysis of urban traffic lights control systems using timed CP-nets," *J. Inf. Sci. Eng.*, vol. 24, no. 3, pp. 875–890, 2008.
[30] Y.-S. Huang and T.-H. Chung, "Modeling and analysis of urban traffic light control systems," *J. Chin. Inst. Eng.*, vol. 32, no. 1, pp. 85–95, 2009.
[31] Y.-S. Huang, Y.-S. Weng, and M. C. Zhou, "Modular design of urban traffic-light control systems based on synchronized timed Petri nets," *IEEE Trans. Intell. Transp. Syst.*, vol. 15, no. 2, pp. 530–539, Apr. 2013.
[32] Y.-S. Huang, Y.-S. Weng, and M. C. Zhou, "Critical scenarios and their identification in parallel railroad level crossing traffic control systems," *IEEE Trans. Intell. Transp. Syst.*, vol. 11, no. 4, pp. 968–977, Oct. 2010.
[33] Y. S. Huang, Y. S. Weng, and M. C. Zhou, "Design of traffic safety control systems for emergency vehicle preemption using timed Petri nets," *IEEE Trans. Intell. Transp. Syst.*, vol. 16, no. 4, pp. 2113–2120, Aug. 2015.
[34] L. Qi, M. C. Zhou, and W. J. Luan, "Emergency traffic-light control system design for intersections subject to accidents," *IEEE Trans. Intell. Transp. Syst.*, vol. 17, no. 1, pp. 170–183, Jan. 2016.
[35] M. P. Fanti, G. Iacobellis, A. M. Mangini, and W. Ukovich, "Freeway traffic modeling and control in a first-order hybrid Petri net framework," *IEEE Trans. Autom. Sci. Eng.*, vol. 11, no. 1, pp. 90–102, Jan. 2014.
[36] J. Q. Wang, J. X. Yan, and L. X. Li, "Microscopic modeling of a signalized traffic intersection using timed Petri nets," *IEEE Trans. Intell. Transp. Syst.*, vol. 17, no. 2, pp. 305–312, Feb. 2016.
[37] A. D. Febbraro, D. Giglio, and N. Sacco, "A deterministic and stochastic Petri net model for traffic-responsive signaling control in urban areas," *IEEE Trans. Intell. Transp. Syst.*, vol. 17, no. 2, pp. 510–524, Feb. 2016.
[38] G. F. List and M. Mashayekhi, "A modular colored stochastic Petri net for modeling and analysis of signalized intersections," *IEEE Trans. Intell. Transp. Syst.*, vol. 17, no. 3, pp. 701–713, Mar. 2016.
[39] L. Qi, M. Zhou and Z. Ding, "Real-time traffic camera-light control systems for intersections subject to accidents: a Petri net approach," in *Proc. SMC*, Oct. 2013, pp. 1069–1074.
[40] P. Roberg, C. R. Abbess, and C. Wright, "Traffic jam simulation," *J. Maps*, vol. 3, no. 1, pp. 107–121, 2007.
[41] G. Liu, "Complexity of the deadlock problem for Petri nets modeling resource allocation systems," *Inf. Sci.*, vol. 363, pp. 190–197, Oct. 2016.
[42] G. J. Liu and C. J. Jiang, "Net-structure-based conditions to decide compatibility and weak compatibility for a class of inter-organizational workflow nets," *Sci. China Inf. Sci.*, vol. 58, no. 7, pp. 1–16, 2015.
[43] X. Lu, M. C. Zhou, A. C. Ammari, and J. C. Ji, "Hybrid Petri nets for modeling and analysis of microgrid systems," *IEEE/CAA J. Autom. Sinica*, vol. 3, no. 4, pp. 349–356, Oct. 2016.
[44] A. Zimmermann, M. Knoke, A. Huck, and G. Hommel, "Towards version 4.0 of TimeNET," in *Proc. 13th GI/ITG Conf. Measuring, Modelling Eval. Comput. Commun. Syst.*, Mar. 2006, pp. 1–4.
[45] C. F. Daganzo, "The cell transmission model: A dynamic representation of highway traffic consistent with the hydrodynamic theory," *Transp. Res. B, Methodol.*, vol. 28, no. 4, pp. 269–287, 1994.
[46] C. F. Daganzo, "The cell transmission model, part II: Network traffic," *Transp. Res. B, Methodol.*, vol. 29, no. 2, pp. 79–93, 1995.
[47] J. Long, Z. Y. Gao, X. Zhao, A. Lian, and P. Orenstein, "Urban traffic jam simulation based on the cell transmission model," *Netw. Spatial Econ.*, vol. 11, no. 1, pp. 43–64, 2011.
[48] M. J. Lighthill and G. B. Whitham, "On kinematic waves. II. A theory of traffic flow on long crowded roads," *Proc. R. Soc. Lond. A, Math. Phys. Sci.*, vol. 229, pp. 317–345, May 1955.
[49] P. I. Richards, "Shock waves on the highway," *Oper. Res.*, vol. 4, no. 1, pp. 42–51, Feb. 1956.

Liang Qi (S'16) received the B.S. and M.S. degrees from Shandong University of Science and Technology, Qingdao, China, in 2009 and 2012, respectively. He is currently working toward the Ph.D. degree with the Department of Computer Science and Technology, Tongji University, Shanghai, China. From 2015 to 2016, he was a joint Ph.D. Student with the Department of Electrical and Computer Engineering, New Jersey Institute of Technology, Newark, NJ, USA. He has authored over a dozen technical papers in journals and conference proceedings. His research interests include Petri nets, intelligent transportation systems, and traffic simulation.

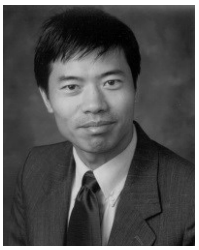

MengChu Zhou (S'88–M'90–SM'93–F'03) received the B.S. degree in control engineering from Nanjing University of Science and Technology, Nanjing, China, in 1983; the M.S. degree in automatic control from Beijing Institute of Technology, Beijing, China, in 1986; and the Ph.D. degree in computer and systems engineering from Rensselaer Polytechnic Institute, Troy, NY, USA, in 1990. He joined the New Jersey Institute of Technology, Newark, NJ, USA, in 1990, where he is currently a Distinguished Professor of Electrical and Computer Engineering. He has authored over 680 publications, including 12 books, over 360 journal papers (over 260 in the IEEE Transactions), and 28 book chapters. His research interests are in Petri nets, manufacturing, transportation, and energy systems. He is a fellow of the International Federation of Automatic Control and American Association for the Advancement of Science.

WenJing Luan (S'16) received the B.S. and M.S. degrees from Shandong University of Science and Technology, Qingdao, China, in 2009 and 2012, respectively. She is currently working toward the Ph.D. degree with the Department of Computer Science and Technology, Tongji University, Shanghai, China. Her research interests include Petri nets, transportation systems and Smart City. She received the Best Student Paper Award-Finalist in the ICNSC 2016 conference.